Hindawi Publishing Corporation
International Journal of Chemical Engineering
Volume 2016, Article ID 9413879, 11 pages
http://dx.doi.org/10.1155/2016/9413879

Research Article

Studies of Adsorption of Heavy Metals onto Spent Coffee Ground: Equilibrium, Regeneration, and Dynamic Performance in a Fixed-Bed Column

N. E. Davila-Guzman,[1] F. J. Cerino-Córdova,[1] M. Loredo-Cancino,[1] J. R. Rangel-Mendez,[2] R. Gómez-González,[1] and E. Soto-Regalado[1]

[1]*Facultad de Ciencias Químicas, Universidad Autónoma de Nuevo León (UANL), Avenida Universidad s/n, Ciudad Universitaria, 66455 San Nicolás de los Garza, NL, Mexico*
[2]*División de Ciencias Ambientales, Instituto Potosino de Investigación Científica y Tecnológica, Camino a la Presa San José 2055, Colonia Lomas 4a Sección, 78216 San Luis Potosí, SLP, Mexico*

Correspondence should be addressed to F. J. Cerino-Córdova; felipejccuanl@yahoo.com.mx

Received 31 December 2015; Revised 7 April 2016; Accepted 11 May 2016

Academic Editor: Iftekhar A. Karimi

Equilibrium and dynamic adsorption of heavy metals onto spent coffee ground (SCG) were studied. The equilibrium adsorption of Cd^{2+}, Cu^{2+}, and Pb^{2+} in a batch system was modeled by an ion-exchange model (IEM) based on an ion-exchange of heavy metals with calcium and protons bonded to active sites on SCG surface. The maximum amount of adsorbed metal ions obtained using the IEM was 0.12, 0.21, and 0.32 mmol/g of Cd^{2+}, Cu^{2+}, and Pb^{2+}, respectively. Regeneration of SCG was evaluated using citric acid, calcium chloride, and nitric acid. The observed trend of desorption efficiency through four adsorption-desorption cycles was HNO_3 > $CaCl_2$ > $C_6H_8O_7$. The effect of process variables such as flow rate and bed height during the dynamic adsorption was evaluated. Moreover, the applicability of a mass transfer model based on external mass transfer resistance, axial dispersion, and ion-exchange isotherm was evaluated, and the results were in good agreement with the experimental data for the adsorption in SCG packed column. The sensitivity analysis of the model parameters showed that axial dispersion coefficient is the most significant parameter in the dynamic simulation. The results obtained showed the potential of SCG as a low-cost material for wastewater metal removal in continuous systems.

1. Introduction

The discharge of heavy metal into environment has increased due to the rapid expansion of industries such as metal plating facilities, fertilizer industries, mining operations, batteries, tanneries, paper industries, and pesticides; heavy metals wastewaters are discharged into the environment increasingly, especially in developing countries. Unlike other contaminants, heavy metals are not biodegradable and tend to accumulate in living organisms, causing various diseases and disorders [1]. Consequently, the treatment of heavy metal containing wastewater is required prior to its discharge. Adsorption with activated carbon is widely recognized as one of the most efficient methods for heavy metal removal at low concentrations from wastewater. However, the use of activated carbon as adsorbent is often limited due to economic reasons; on the other hand, biosorbents are inexpensive and exhibit some selectivity for heavy metals [2]. Consequently, the use of agroindustrial wastes for the heavy metal adsorption from aqueous solutions has been investigated in several studies [3]. According to the US Department of Agriculture, the world coffee production forecast for 2015-2016 is 9.162×10^9 kg [4]. The coffee beverage industry generates large quantities of spent coffee ground as waste, which was previously used as biosorbent of heavy metals [5–7]. The spent coffee ground was used as an adsorbent in this research due to low cost, high availability, and the functional groups of the organic compounds (polysaccharides, flavonoids, alkaloids,

etc.) present in its structure [3], which are able to adsorb and/or interchange metal ions.

One of the main drawbacks of adsorption is the pollution generated by the disposal of the spent adsorbent. To overcome this disadvantage, there are numerous adsorbent regeneration methods used to reestablish the maximum adsorbent capacity and to preserve, as much as possible, the initial weight and pore structure of the adsorbent. Chemical regeneration of adsorbents is a feasible method that has some advantages; for instance, it can be performed in situ, there are no losses of adsorbent, it is possible to recover valuable adsorbates, and the chemical reagents can be reused [8].

For predicting the viability of an adsorbent, it is critical to develop models and experimental procedures that could be used for accurately describing the dynamics of the pollutant adsorption under a variety of operating conditions from lab scale measurements. This requires knowing one or more parameters determined in a stirred-batch system and in short bed laboratory experiments that fairly reproduce the behavior of full-scale adsorbers [9]. Therefore, the objective of this study is to investigate the ability of spent coffee ground to remove Cd^{2+}, Cu^{2+}, and Pb^{2+} ions from aqueous solutions in a continuous system (fixed-bed column). In a previous study, the physicochemical characterization of the SCG was determined, and the adsorption mechanism was elucidated as ion-exchange between the calcium and protons on the adsorbent surface and copper ions. In addition, the rate-controlling rate was found to be the external mass transfer [5]. Thus, the adsorption isotherm was simulated by a proposed ion-exchange multicomponent model and the maximum amount of adsorbed heavy metals was obtained. Furthermore, the effect of different eluents was evaluated in four adsorption/desorption cycles. In dynamics adsorption experiments, the effects of flow rate and bed height were evaluated in order to increase the adsorption capacity and the breakthrough time. Finally, a mass transfer model that includes external mass transfer resistance, axial dispersion, and ion-exchange isotherm was used to predict the adsorption of heavy metals in a fixed bed of spent coffee ground.

2. Materials and Methods

2.1. Biosorbent and Metal Solution. Spent coffee ground (SCG) was collected locally from coffee makers as a waste material. The SCG were washed with deionized water and dried at room temperature. A chemical modification with NaOH was carried out following the procedure described in a previous study [5]. Cd^{2+}, Cu^{2+}, and Pb^{2+} solutions were prepared by dissolving appropriate amounts of $Cd(NO_3)_2{\cdot}4H_2O$, $Cu(NO_3)_2{\cdot}2.5H_2O$, and $Pb(NO_3)_2$, respectively, from stock solutions. All reagents used in this study were of analytical-reagent grade and supplied by Sigma-Aldrich. The cadmium, copper, and lead concentrations were measured at 228.8, 324.7, and 217 nm wavelength, respectively, by using a flame atomic absorption spectrometer with an air/acetylene flame (Thermo Scientific®). Previous to concentration analysis, curve calibration was obtained by measuring the absorbance of different standard solutions of heavy metal ions with known concentration and by following the Beer-Lambert Law.

2.2. Adsorption Batch Experiments. Batch adsorption experiments were carried out in a cage-reactor system [10]. A fixed amount of SCG (0.75 g) placed in the reactor cage was hydrated with acidic water (pH 4.5) to swell the adsorbent. After 12 h of hydration, the reactor cage was removed and the acidic water solution was replaced by 750 mL of metallic solution at 0.1–1.0 mM initial meal concentration. Then, the reactor cage with the SCG was added to the metallic solution at 25°C and the stirrer was turned on at 400 min^{-1}. From a previous study [5], the pH was fixed at 4.5 in order to increase the affinity of the adsorbate and the adsorbent since lead and copper ions precipitate at pH > 5.5 and the surface charge of the adsorbent is predominantly negative at pH > 3.8 (ZPC). During the adsorption process, the pH solution was kept constant at 4.5 by adding 0.1 mM NaOH. In addition, the cage-reactor system was sealed with paraffin film in order to avoid losses by water evaporation. Several samples were taken from the solution in order to analyze the ion metal concentration by flame atomic absorption spectrometer (Thermo Scientific). The equilibrium adsorption capacity was evaluated at different initial ion metal concentration (0.1–1 mM). The amount of metal ion adsorbed at equilibrium, q_e, was calculated taken into account the volume of each sample use in the chemical analysis as follows:

$$q_e = \frac{V_o C_o - (V_o - V_s + V_a) C_e}{m_{\mathrm{SCG}}}, \quad (1)$$

where C_o and C_e are the initial and equilibrium ion metal concentration in mmol/L, respectively; V_o is the initial solution volume in L; V_s is the volume taken for the ion metal concentration analysis in L; V_a is the NaOH added volume due to the pH control in L; m_{SCG} is the dry weight of SCG in g; q_e is the adsorption capacity at equilibrium in mmol/g.

The regeneration of the SCG was determined through four adsorption-desorption cycles. For the adsorption process, the same procedure described before was followed. In the desorption process, the metal loaded-SCG was in contact with 750 mL of 0.1 M eluent solution (citric acid, calcium chloride, or nitric acid) and several aliquots were taken at various time intervals in order to analyze the ion metal concentration. After each desorption process new ion metal solution (0.1 mM) was added to carry out a new adsorption process. The desorption capacity (q_{des}) was calculated by the difference between the adsorption capacity and the ion metal quantity released after the desorption process per mass of SCG:

$$q_{\mathrm{des}} = q - \frac{(V_e - V_s) C}{m_{\mathrm{SCG}}}, \quad (2)$$

where V_e is the initial volume of the eluent in L, V_s is the volume taken for the ion metal concentration analysis in L, q is the adsorption capacity in mmol/g, m_{SCG} is the SCG mass in g, and C is the ion metal concentration after the desorption process in mmol/L.

2.2.1. Ion-Exchange Model. Previous studies have demonstrated that the adsorption mechanism of Cu^{2+} onto the SCG could be established as an ion-exchange reaction type between cations (Ca^{2+}) and protons (H^+) initially bound to the SCG and the copper ions present in the aqueous phase (M^{2+}) [5]. In this study, an ion-exchange model was adapted from Diniz et al. (2008) [11], in the model proposed in this paper Ca^{2+} and protons exchanged by M^{2+} were represented by the following exchange reaction:

$$M^{2+} + 2HB \longleftrightarrow MB_2 + 2H^+ \quad (3)$$

$$M^{2+} + CaB_2 \longleftrightarrow MB_2 + Ca^{2+} \quad (4)$$

where M^{2+} is the metal ion (Cd^{2+}, Cu^{2+}, or Pb^{2+}), HB are the protonated adsorption sites, B are the adsorption sites (i.e., hydroxyl, carboxyl groups), and CaB_2 are the neutralized adsorption sites with calcium ions.

Using the separation factors (α_i^j) and the law of conservation of mass, the ion-exchange multicomponent model was obtained:

$$y_M = \frac{\alpha_{Ca}^M \alpha_H^M x_M}{x_M\left(\alpha_{Ca}^M \alpha_H^M - \alpha_H^M\right) + x_H\left(\alpha_H^M + \alpha_{Ca}^M\right) + \alpha_H^M}, \quad (5)$$

where α_H^M and α_{Ca}^M are the separations factor between the metal ion and the proton and between the metal and the calcium ions, respectively.

The equivalent fraction of metal ions in liquid phase (x_M) and the equivalent fraction in the solid phase (y_M) were obtained as follows:

$$x_i = \frac{C_i}{C^\circ}, \qquad y_i = \frac{q_i}{Q_s}, \quad (6)$$

where C_i is the ion metal concentration in the liquid phase (meq/L), C° is the total initial concentration of the liquid solution (meq/L), q_i is the ion metal amount per gram of SCG (meq/g), and Q_s is the amount of active sites per gram of SCG (meq/g).

The equilibrium model parameters (Q_s and α_i^j) were evaluated by nonlinear regression minimizing the mean squared error function (MSE):

$$\mathrm{MSE} = \frac{1}{N}\sum_{i=1}^{N}\left(q_i^* - q_i\right)^2. \quad (7)$$

2.3. Adsorption Column Experiments. The breakthrough curves were carried out in a borosilicate column of 1 cm internal diameter and 30 cm height. A specified amount of SCG was hydrated with acidic water (pH 4.5) during 12 h in conical flask of 50 mL at 25°C and 200 min^{-1} in an orbital shaker. After filtering the SCG, the column was packed. Then, acidified water (pH = 4.5) was passed at 4 mL/min flow rate until the effluent pH was 4.5 (approximately 20 min). The excess of water was drained from the bottom of the column without allowing the liquid level to drop below the bed height in order to avoid air bubbles formation. The feed solution containing the total metal concentration of 0.1 mM was pumped downward through the column. The initial pH was 4.5 and the temperature was 25°C. The effect of flow rate in metal ion removal was studied in a column with 14 cm bed height (i.e., 2 g of SCG) at different volumetric flow rates (5.5, 7.7, 11, and 22 mL/min). In order to determine the effect of the bed height on the ion metal removal, the breakthrough curves were obtained at three different bed heights at a constant flow rate of 5.5 mL/min. The column was packed with 2, 4, and 8 g of SCG equivalent to 7, 14, and 21 cm of bed height, respectively.

The total quantity of metal adsorbed in the SCG (m_{ads}) was calculated from the area below the breakthrough curve multiplied by the flow rate. The adsorption capacity was obtained from the ratio of m_{ads} to m_{SCG}.

2.3.1. Mass Transfer Column Model. The adsorption process performed in a continuous system is one of the most important processes in wastewater treatment [12]. The knowledge of the concentration-time profile (breakthrough curve) is required for the design of an adsorption column. A mathematical model could be used for simulation of breakthrough curves. Assuming isothermal conditions, constant physical properties for the feed solution, axial dispersion, and a linear driving force for the solid phase rate-controlling step, the mass balance in the liquid and solid phases gives the subsequent equations:

$$\frac{\partial x_M}{\partial \tau} + \frac{\partial x_M}{\partial \xi} + \frac{\rho Q}{\varepsilon_b C^\circ}\frac{\partial y_M}{\partial \tau} = \frac{1}{\mathrm{Pe}}\frac{\partial^2 x_M}{\partial \xi^2}, \qquad \frac{\partial y_M}{\partial \tau} = \frac{K_T L S C^\circ}{Q \upsilon \rho}\left(x_M - x_M^*\right) \quad (8)$$

with the following initial and boundary conditions:

$$x_M = 1, \quad \xi = 0; \qquad \frac{\partial x_M}{\partial \xi} = 0, \quad \xi = 1; \quad (9)$$

$$x_M = 0, \quad y_M = 0. \quad (10)$$

The dimensionless variables are also introduced as follows:

$$\tau = \frac{t\upsilon}{L\varepsilon_b}; \qquad \xi = \frac{Z}{L}; \qquad x_M = \frac{C_M}{C^\circ}; \qquad y_M = \frac{y_M}{Q_s}, \quad (11)$$

where K_T is the external mass transfer coefficient (cm/min), S is the superficial particle area per volume (0.0758 cm^{-1}), L is the packed bed length (cm), Q is the flow rate (cm^3/min), ρ is the particle density (747 g/cm^3), υ is the interstitical velocity (cm/min), ε_b is the bed porosity (0.40), Pe is the Peclet number, x_M^* is the equilibrium equivalent fraction obtained from the ion-exchange multicomponent model (mmol/L), and x_M is the equivalent fraction of the ion metal at the time t. The partial differential equations were solved numerically by using finite difference method and Fortran software.

The Sherwood number was used to determine the external mass transfer coefficient by the following equations:

$$\mathrm{Sh} = \frac{1.09}{\varepsilon_b}\mathrm{Re}^{1/3}\mathrm{Sc}^{1/3}$$
$$K_T = \frac{\mathrm{Sh}D^\circ_{\mathrm{AB}}}{2R_p}, \tag{12}$$

where Re and Sc are the Reynolds and Schmidt numbers, R_p is the particle diameter (cm), and D°_{AB} is the diffusion coefficient (cm^2/s) obtained by using the Nernst-Haskell equation:

$$D^\circ_{\mathrm{AB}} = \frac{RT\left[\left(1/z_+\right)+\left(1/z_-\right)\right]}{F^2\left[\left(1/\lambda^\circ_+\right)+\left(1/\lambda^\circ_-\right)\right]}, \tag{13}$$

where R is the ideal gas constant (8.314 J/mol K), F is the Faraday constant (96,500 C/mol), z is the ionic valence, λ° is the limiting ionic conductance (Scm^2/mol) [13].

The axial dispersion coefficient (D_L) was obtained by the Peclet number which was calculated by the following empirical correlation [14]:

$$\mathrm{Pe} = \frac{0.2 + 0.011\mathrm{Re}^{0.48}}{\varepsilon_b},$$
$$\mathrm{Pe} = \frac{L\upsilon}{D_L}. \tag{14}$$

In addition, model sensitivity analysis was conducted to reveal the effect of the model parameters (affinity constant, external mass transfer, and axial dispersion coefficient) on the breakthrough curves simulations [15, 16]. The relative significance of the model parameters can be identified by plotting the relative change of the value of interest (dx/x) against the relative change in the value of the parameter under investigation (dy/y) [17]:

$$\%\frac{dx}{x} = \frac{x_i - x_{\mathrm{ref}}}{x_{\mathrm{ref}}} \times 100\%, \tag{15}$$

$$\%\frac{dy}{y} = \frac{y_i - y_{\mathrm{ref}}}{y_{\mathrm{ref}}} \times 100\%. \tag{16}$$

The reference values for the axial dispersion, external mass transfer coefficients, and the affinity constant (x_{ref}) were obtianed from (15), (16), and (5), respectively. Furthermore, the performance of the mass transfer model was evaluated by using (7), where q_i^* is the experimental adsorpiton capacity and q_i is the adsorption capacity estimated by the mass transfer model.

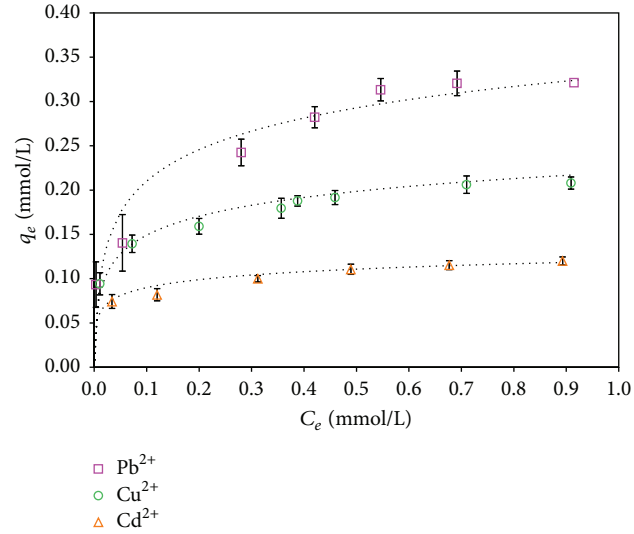

Figure 1: Isotherm adsorption of Cd^{2+}, Cu^{2+}, and Pb^{2+} onto SCG. Experimental conditions: 1 g SCG/L, pH 4.5, and 25°C. Solid lines represent the ion-exchange multicomponent model. Error bars represent standard deviation of triplicate measurements.

Table 1: Maximum adsorption capacities of heavy metals onto various adsorbents reported in literature.

Adsorbent	q (mmol/g)			pH	Ref.
	Cd^{2+}	Cu^{2+}	Pb^{2+}		
Amberlite IR-120	0.90	0.34	0.41	NR	[26]
Dowex 50 W	0.25	0.35	0.23	8	[19]
Powdered activated carbon	0.10	0.52	0.17	7	[27]
Granular activated carbon	0.03	0.08	0.08	5	[18]
Tea waste	—	0.75	0.31	NR	[28]
SCG	0.12	0.21	0.32	4.5	*This work*
Olive stone waste	0.15	0.09	0.14	5	[29]
Coffee ground	0.10	0.03	0.24	5	[30]

NR: not reported.

3. Results and Discussions

3.1. Equilibrium Adsorption of SCG. The equilibrium adsorption studies were carried out in order to obtain the maximum adsorption capacity of Cd^{2+}, Cu^{2+}, and Pb^{2+} onto SCG (Figure 1). The isotherms are concave with respect to the equilibrium concentration axis (C_e), indicating a favorable isotherm. There is a fast increment of the equilibrium adsorption capacity with the augmentation of C_e values until a horizontal saturation plateau is reached. The maximum adsorption capacities were 0.12, 0.21, and 0.32 mmol/g of Cd^{2+}, Cu^{2+}, and Pb^{2+}, respectively. These adsorption capacities were compared with those reported in literature for other adsorbents (Table 1). The maximum amount of adsorbed Cd^{2+}, Cu^{2+}, and Pb^{2+} ions was 4, 2.63, and 4 times greater than that reported by using granular activated carbon [18]. However, it is important to mention that the adsorption capacities reported in this study were 7.5, 1.62, and 1.28 times lower than those reported by using ion-exchange resins [19].

Table 2: Parameters and error values of the ion-exchange multicomponent model for the adsorption of heavy metals onto SCG.

Parameters	Cd^{2+}	Cu^{2+}	Pb^{2+}
Q_s (mmol/g)	0.12	0.23	0.32
α_H^M	2.88	4.78	12.00
α_{Ca}^M	1.62	4.52	7.00
MSE ($\times 10^5$)*	*9.10*	*17.00*	*37.50*

*MSE: mean squared error.

Nevertheless, the high cost of the ion-exchange resins (≈$3,000/kg) is a serious disadvantage for their application in wastewater treatment.

The equilibrium data were analyzed due to its relevance in the development of an equation that could be used for design purposes. A mathematical model that takes into consideration an ion-exchange mechanism for the adsorption of heavy metals was used in order to predict the adsorption capacity of the SCG as a function of the equilibrium concentration of the heavy metals. The adsorption capacities predicted by the ion-exchange model are shown in Table 2. The model predicted well the equilibrium data according to the low error values (MSE < 37.5×10^{-5}). The separation factors are greater than the unit, indicating that the SCG has a stronger affinity for the heavy metals than protons and calcium ions, favoring the adsorption of Cd^{2+}, Cu^{2+}, and Pb^{2+}. On the other hand, there is a general trend observed in the affinity constant values ($\alpha_H^M > \alpha_{Ca}^M$); these results suggest that the proton is exchanged by the ion metal more easily than by the calcium ions. This could be explained considering that the separation factor is function of the ionic charge and the hydrated ionic radius. The affinity of the SCG for the metal ions over the protons could be due to the ionic charge, since the metal ions have a charge (+2) whereas the protons have a charge (+1). However, there is no difference in the ionic charge between the metal ions and the calcium ions. The preference of the SCG for the metal ions over the calcium ions could be attributed to the lower hydrated ionic radius of the metal ions. The hydrated ionic radii of Cd^{2+}, Cu^{2+}, and Pb^{2+} are 0.426, 0.419, and 0.401 nm, respectively, whereas the hydrated ionic radius of Ca^{2+} is 0.642 nm [20].

3.2. Desorption of Heavy Metals from SCG. The regeneration process is an important aspect for the efficiency of an adsorbent in wastewater treatments [21]. For this reason, the regeneration of the SCG was evaluated using three different eluents: an organic acid (citric acid), an inorganic acid (nitric acid), and an inorganic salt (calcium chloride). Four adsorption-desorption cycles were carried out at 0.1 mM initial metal concentration and 0.1 M concentration of the eluent. Additionally, the speciation diagrams, obtained from the Medusa/Hydra software package, were used in order to understand the interaction between the eluent and the heavy metals during the desorption process.

3.2.1. Desorption of Heavy Metals with Citric Acid. The desorption of Cu^{2+} and Pb^{2+} with citric acid during four adsorption-desorption cycles is shown in Figure 3. The desorption capacity of the citric acid was 0.059 mmol Pb^{2+}/g SCG during three adsorption-desorption cycles. After three cycles, the desorption capacity of the citric acid decreased to 0.050 mmol Pb^{2+}/g SCG. Moreover, the citric acid was able to desorb all the Cu^{2+} adsorbed onto SCG during four adsorption-desorption cycles.

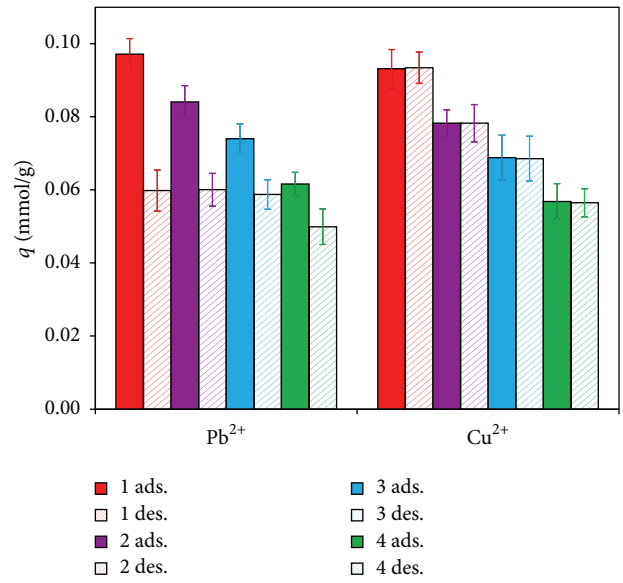

Figure 2: Adsorption-desorption cycles of Pb^{2+} and Cu^{2+} using citric acid. Experimental conditions: 0.1 mM initial metal concentration, pH 4.5, and 25°C. Error bars represent standard deviation of triplicate measurements.

The speciation diagrams of the citrate ions with Pb^{2+} and Cu^{2+} reveal that the free fraction of Pb^{2+} is 0.392, suggesting that only 60.8% of the Pb^{2+} ions could form a complex with the citrate ions. This percentage of complexation is similar to the average desorption percentage of Pb^{2+} obtained with citric acid (64.5%). On the other hand, the free fraction of Cu^{2+} is 9.1×10^{-3}, indicating that 99.09% of Cu^{2+} could form a complex with citrate ions. Although citric acid shows high desorption capacities, its performance as eluent is not adequate due to the decrease of the adsorption capacity of the SCG after each desorption cycle (Figure 2).

3.2.2. Desorption of Heavy Metals with Calcium Chloride. The desorption of heavy metals from the SCG was evaluated using 0.1 M $CaCl_2$ as eluent. In Figure 3, the adsorption and desorption capacities of Cu^{2+} and Pb^{2+} during four adsorption-desorption cycles are shown. The calcium chloride was able to desorb 76.58% of Pb^{2+} ions with an average desorption capacity of 0.076 mmol/g, whereas the desorption percentage of Cu^{2+} was 62% with an average desorption capacity of 0.057 mmol/g.

The desorption capacity of calcium chloride was higher for Pb^{2+} than for Cu^{2+} ions, due to the fact that calcium chloride forms more complex with Pb^{2+} (3) than Cu^{2+} (2), according to the speciation diagrams. The adsorption capacity of

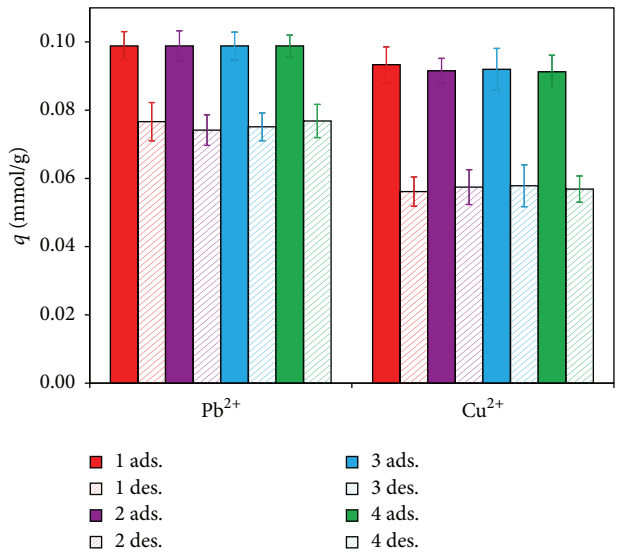

Figure 3: Adsorption-desorption cycles of Pb^{2+} and Cu^{2+} using calcium chloride. Experimental conditions: 0.1 mM initial metal concentration, pH 4.5, and 25°C. Error bars represent standard deviation of triplicate measurements.

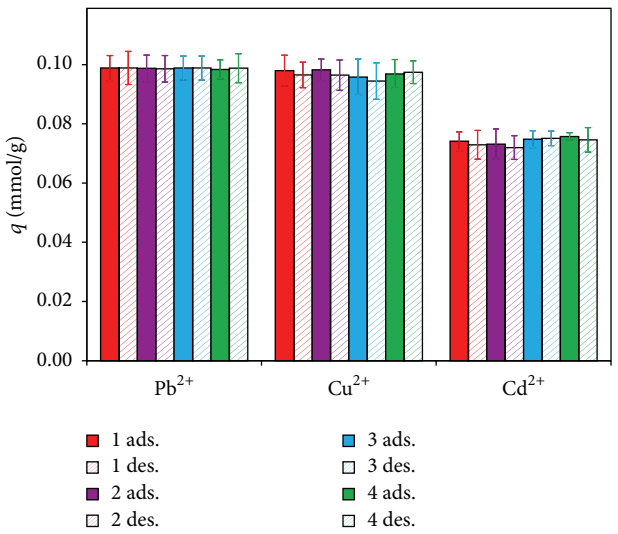

Figure 4: Adsorption-desorption cycles of Pb^{2+}, Cu^{2+}, and Cd^{2+} using nitric acid. Experimental conditions: 0.1 mM initial metal concentration, pH 4.5, and 25°C. Error bars represent standard deviation of triplicate measurements.

Pb^{2+} and Cu^{2+} after each desorption cycle was not affected by the interaction between the calcium chloride and the SCG, since the calcium ions could act as regeneration agent neutralizing the active sites in the surface of the SCG.

3.2.3. Desorption of Heavy Metals with Nitric Acid. The desorption of the heavy metals was evaluated using 0.1 M HNO_3 as eluent. The desorption kinetics were performed in order to evaluate the weight loss of the adsorbent material for the possible chemical attack of the high ionic strength of the nitric acid. Previous studies showed that the contact time necessary to achieve the complete desorption of the heavy metals was 10 min and a desorption percentage was greater than 97% (data not shown). Furthermore, there was no weight loss of SCG during the desorption process. The nitric acid was chosen as the eluent for the desorption of Cd^{2+}, Cu^{2+}, and Pb^{2+} due to its high desorption efficiency.

Four adsorption-desorption cycles were carried out with 0.1 M HNO_3 as eluent (Figure 4). The desorption of the metal ions was 100% during four desorption cycles and the average desorption capacities were 0.074, 0.096, and 0.099 mmol/g for Cd^{2+}, Cu^{2+}, and Pb^{2+}, respectively. The adsorption capacity of the SCG after each adsorption-desorption cycle was the same, indicating that the SCG was not affected by the interaction with the inorganic acid. The desorption capacity of the nitric acid could be attributed to the high quantity of protons in the solution, which can displace the metal ions initially adsorbed onto the SCG from the adsorption sites. Moreover, the ion-exchange of the metal ions by the protons could allow the regeneration of the SCG surface by the protonation of the adsorption sites. This regeneration enabled having the same adsorption capacity of the SCG as in the first adsorption cycle, when the adsorbent was not in contact with the eluent.

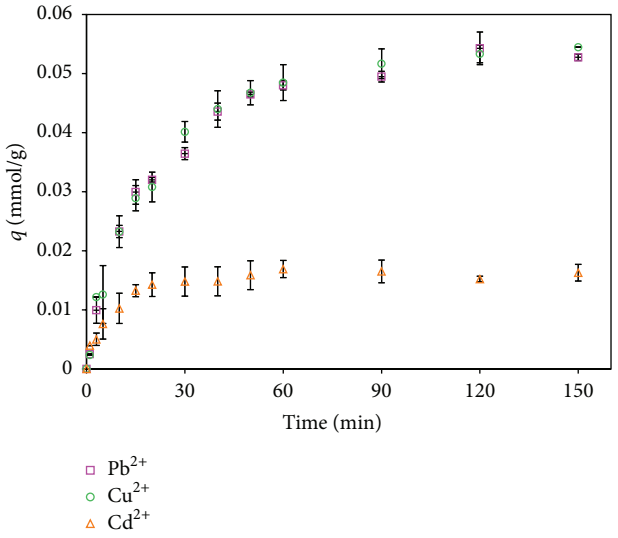

Figure 5: Equimolar multicomponent adsorption kinetics of SCG. Experimental conditions: 0.1 mM initial equimolar metal concentration, pH 4.5, and 25°C. Error bars represent standard deviation of triplicate measurements.

3.3. Multicomponent Adsorption. Most of the industrial processes generate effluents with more than one metal ion [22]. For this reason, the adsorption capacity of the SCG on the removal of Cd^{2+}, Cu^{2+}, and Pb^{2+} in multicomponent system was evaluated at an equimolar initial metal concentration (0.1 mM) and constant pH 4.5 (Figure 5). The adsorption capacity of Cu^{2+} and Pb^{2+} was 0.054 and 0.053 mmol/g, respectively, while the adsorption capacity of Cd^{2+} was 0.0163 mmol/g. The adsorption capacity of Cu^{2+} and Pb^{2+} onto SCG in the multicomponent system was 44.8% lower than that obtained in the individual systems. On the other

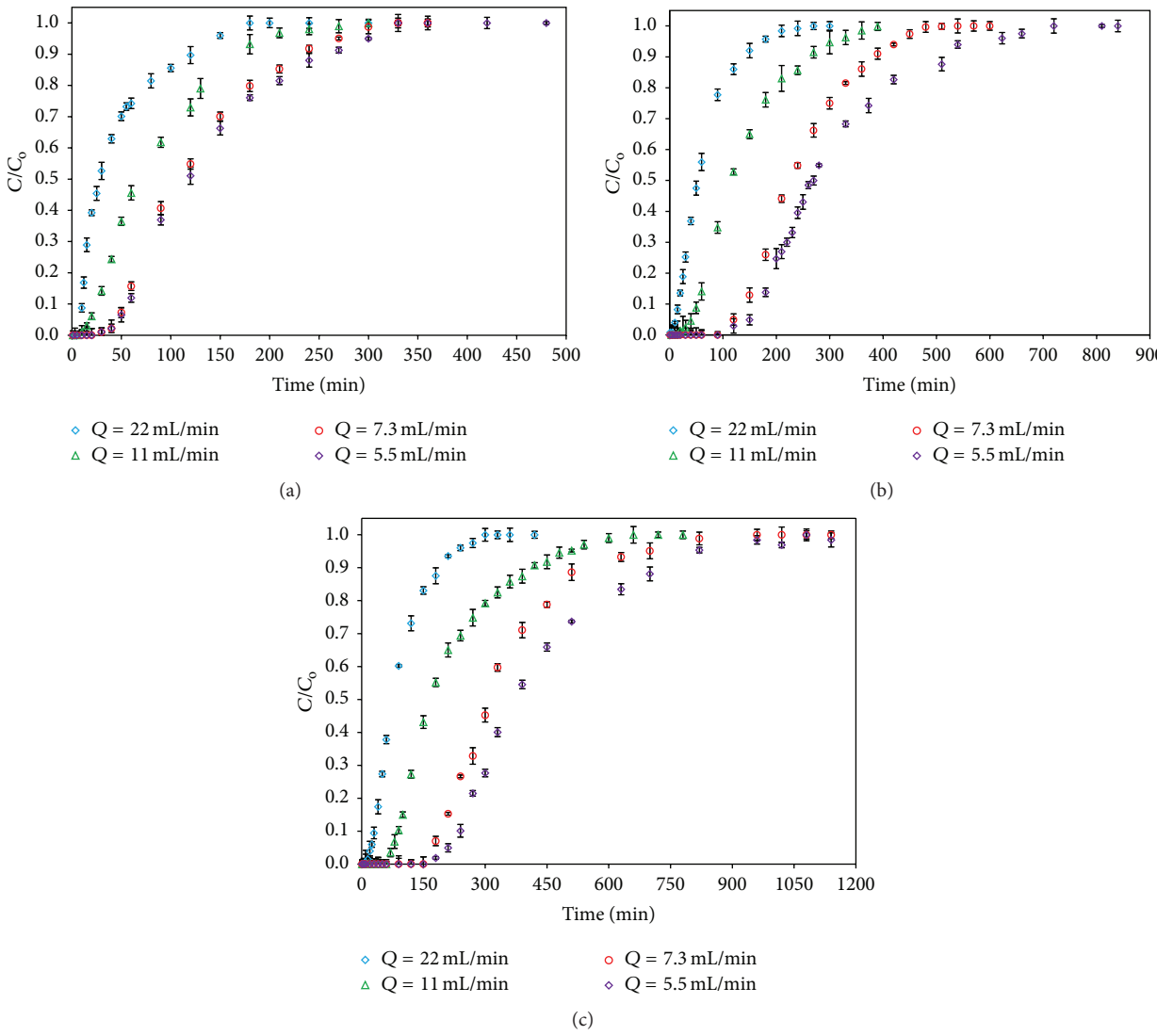

FIGURE 6: Effect of the flow rate on the breakthrough curves of (a) Cd^{2+}, (b) Cu^{2+}, and (c) Pb^{2+}. Experimental conditions: 0.1 mM initial metal concentration, pH 4.5, and 25°C.

hand, the adsorption of Cd^{2+} onto SCG in the multicomponent system was 78.4% lower than the adsorption in the individual system. This behavior could be attributed to the competition between the metal ions for the same adsorption sites. Moreover, this competition increased the contact time to reach the saturation by 3 times for the Cu^{2+} and Pb^{2+} adsorption (120 min) compared with the saturation time in the individual systems (40 min). Meanwhile, the saturation time for the adsorption of Cd^{2+} is not influenced by the presence of other ions in the aqueous solution. Additionally, the total adsorption of the SCG in the multicomponent system increased from 0.097 mmol/g (individual system) to 0.124 mmol/g, corresponding to the sum of the adsorption capacity of the heavy metals in the multicomponent system. The increase in the adsorption capacity could be attributed to different affinities of the heavy metal ions for the adsorption sites on the SCG.

3.4. Breakthrough Curves of Heavy Metals onto SCG. The effect of the bed height and the flow rate were evaluated in order to obtain the breakthrough time and the adsorption efficiency in the range of experimental conditions studied. The breakthrough curves of Cd^{2+}, Cu^{2+}, and Pb^{2+} were obtained at different flow rates of 5.5, 7.3, 11, and 22 mL/min and initial metal concentration of 0.1 mM (Figure 6). The breakthrough time was established as the time necessary to reach an effluent concentration of 0.007 mmol/L as defined in environmental regulations [23]. As can be seen in Figure 6, the breakthrough time increased with the decrease of the flow rate. The maximum breakthrough times were 50, 160, and 220 min for the adsorption of Cd^{2+}, Cu^{2+}, and Pb^{2+}, respectively; and the corresponding adsorption capacities were 0.0373, 0.0838, and 0.135 mmol/g, obtained at the lowest flow rate (5.5 mL/min). As the flow rate decreased, the residence time of the metal ions increased which

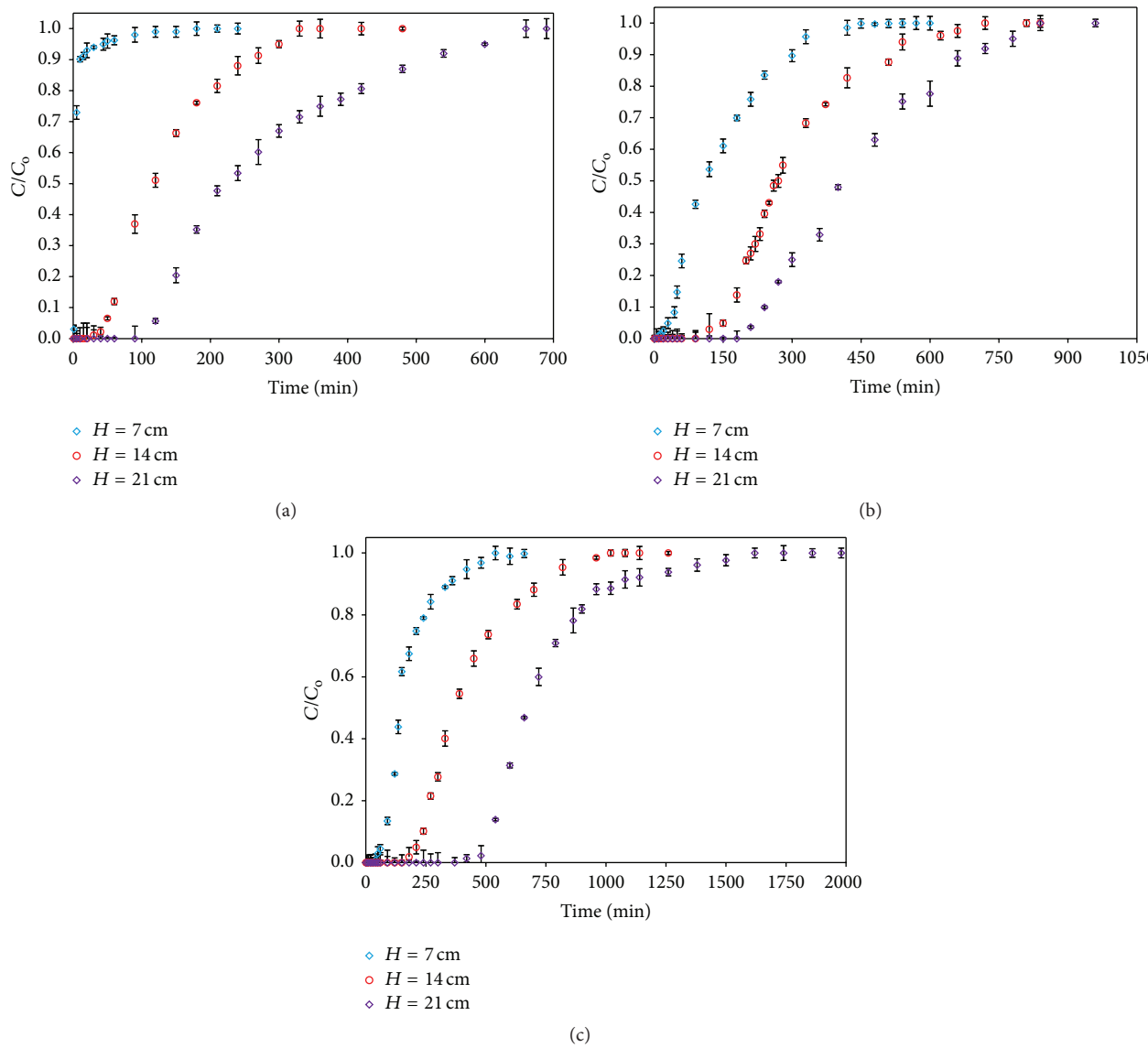

FIGURE 7: Effect of the bed height on the breakthrough curves of (a) Cd^{2+}, (b) Cu^{2+}, and (c) Pb^{2+}. Experimental conditions: 0.1 mM initial metal concentration, pH 4.5, and 25°C.

results in a longer contact time between the heavy metals and the SCG. However, the higher adsorption capacity of Cd^{2+} (0.0496 mmol/g), Cu^{2+} (0.0894 mmol/g), and Pb^{2+} (0.171 mmol/g) was obtained at the flow rate of 7.3 mL/min. This behavior could be attributed to the phenomenon of the axial dispersion, which has been reported in literature to be more significant at low flow rates [24], reducing the efficiency of the dynamic adsorption in fixed-bed columns.

Additionally, the effect of the bed height in the breakthrough time and the adsorption capacity was evaluated at 7, 14, and 21 cm. The breakthrough curves were obtained at 0.1 mM initial metal concentration, initial pH of 4.5, and 5.5 mL/min flow rate (Figure 7). Figure 7 reveals that the higher breakthrough time is obtained at the higher bed height. As the bed height increases from 7 to 21 cm, the breakthrough time for the adsorption of Cu^{2+} and Pb^{2+} increases 5.75 and 6.25 times, respectively, whereas the breakthrough time for the adsorption of Cd^{2+} increases from 0 to 130 min, when the bed height is increased from 7 to 21 cm. As the bed height is increased, the amount of adsorbent also increased, which means a higher amount of functional groups available for the heavy metal adsorption. The adsorption capacities obtained at the highest column height were 0.067, 0.103, and 0.202 mmol/g for the adsorption of Cd^{2+}, Cu^{2+}, and Pb^{2+}, respectively.

3.5. Mathematical Modeling. The breakthrough curves were simulated using a mass transfer model that includes axial dispersion, external mass transfer resistance, and ion-exchange isotherm model. The experimental conditions were 0.1 mM initial metal concentration, 5.5 mL/min flow rate, and 14 cm bed height. As shown in Figure 8, the mass transfer model was

Table 3: External mass transfer and axial dispersion coefficients for heavy metal adsorption onto SCG.

Metal	λ° (Scm^2/mol)	D°_{AB} (m^2/s)	K_T (m/s)	α^{M}_{Ca}	MSE
Cd^{2+}	108.13	1.71×10^{-9}	1.07×10^{-5}	1.62	0.017
Cu^{2+}	107.20	1.72×10^{-9}	1.08×10^{-5}	4.52	0.012
Pb^{2+}	142.00	1.89×10^{-9}	1.14×10^{-5}	7.00	0.017

The axial dispersion coefficient (D_L) was taken as constant at 3.53×10^{-6} m^2/s.

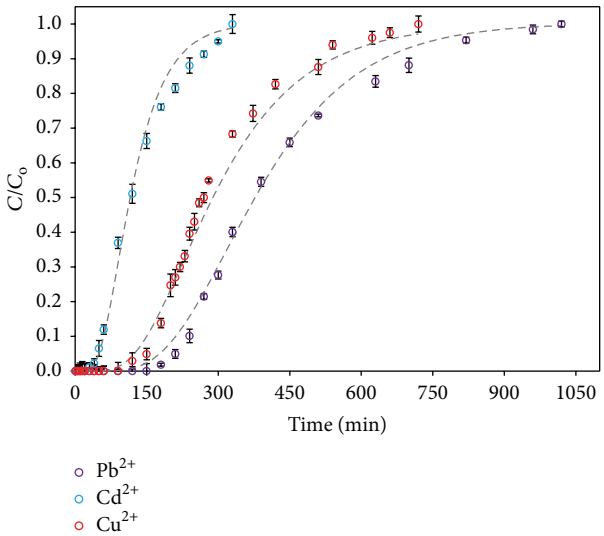

Figure 8: Mass transfer model for heavy metal adsorption onto SCG. Experimental conditions: 0.1 mM initial metal concentration, 14 cm bed height, 5.5 flow rate, and 25°C. Dashed lines represent the mass transfer model.

able to predict well the breakthrough curves of Cd^{2+}, Cu^{2+}, and Pb^{2+} from the initial time until the saturation time. The error values obtained for the simulation of the breakthrough curves of the heavy metals onto SCG were lower than 0.42 (Table 3) indicating a good performance of the mass transfer model. The mass transfer model provides important information about the performance of the breakthrough curves. For instance, the external mass transfer coefficient for Pb^{2+} adsorption was the highest compared to the Cd^{2+} and Cu^{2+} adsorption. This could be associated at faster diffusion of the ions through the stagnant film which surrounded the SCG particles. Furthermore, the affinity constant for the adsorption of Pb^{2+} was the highest compared to the values obtained for the adsorption of Cd^{2+} and Cu^{2+}. These results indicate that the adsorption of Pb^{2+} onto SCG in a fixed-bed column is more efficient than the adsorption of Cd^{2+} and Cu^{2+}, which are consistent with the experimental results obtained in Section 3.1.

The relative importance of the model parameters in the prediction of the breakthrough time was determined by varying one parameter at the time (e.g., axial dispersion coefficient, external mass transfer coefficient, and affinity constant) while maintaining the rest of the parameters fixed. The sensitivity analysis of the mass transfer model is shown in Figure 9. The model parameter with the highest influence on the breakthrough time was the axial dispersion coefficient (D_L) in comparison with the external mass transfer coefficient and the affinity constant. The increase of D_L by 50% caused a decrease in the breakthrough time of 16.4% for the Pb^{2+} adsorption and 21.78% for the Cd^{2+} and Cu^{2+} adsorption, with respect to the reference values (Table 3). A further increase in D_L (90%), produced diminution in the breakthrough times of 185.65, 206.28, and 246.23% in the adsorption of Cd^{2+}, Cu^{2+}, and Pb^{2+}, respectively. However, when D_A is decreased even by 90%, the effect in the breakthrough time is minimum with an increment lower than 10%. The effect of the axial dispersion has been established in literature, where low values of D_L are required in order to obtain a high performance of the fixed-bed column.

The sensitivity analysis of the external mass transfer coefficient (K_T) shows that the increment in this parameter has a small effect in the breakthrough time. For example, when K_T was increased to 33% the breakthrough time had an increment of 3.5, 7.65, and 13.25% in the adsorption of Cd^{2+}, Cu^{2+}, and Pb^{2+}, respectively. On the other hand, the decrement of K_T by 70% produced a decrease in the breakthrough times of 15.1, 28.85, and 36.25% in the adsorption of Cd^{2+}, Cu^{2+}, and Pb^{2+}, respectively. The reduction in the external mass transfer coefficient is equivalent to an increment in the mass transfer resistance, causing earlier breakthrough times.

Additionally, the sensitivity analysis of the affinity constant showed that even a small increase in the parameter of 10% can cause an increment in the breakthrough times of 17.58, 22.52, and 26.59% for the adsorption of Cd^{2+}, Cu^{2+}, and Pb^{2+}, respectively. An increase in the affinity constant implies an increment in the affinity between the SCG and the metal ions. This increase could be obtained by the modification of the surface of the SCG that could generate more active sites for the heavy metal adsorption [25].

According to the sensitivy analysis, the mass transfer model is more sensitive to the axial dispersion coefficient than the affinity contast and even more than the external mass transfer coefficient. These results demonstrate that the axial dispersion is a significant phenomenon in the behavior of the breakthrough curves of Cd^{2+}, Cu^{2+}, and Pb^{2+} onto SCG.

4. Conclusions

The present study shows that spent coffee ground is able to remove heavy metals from aqueous solutions. The model proposed of ionic exchange predicts well the experimental data, and this model represents the ion-exchange of the heavy metals by the protons and calcium ions bonded to

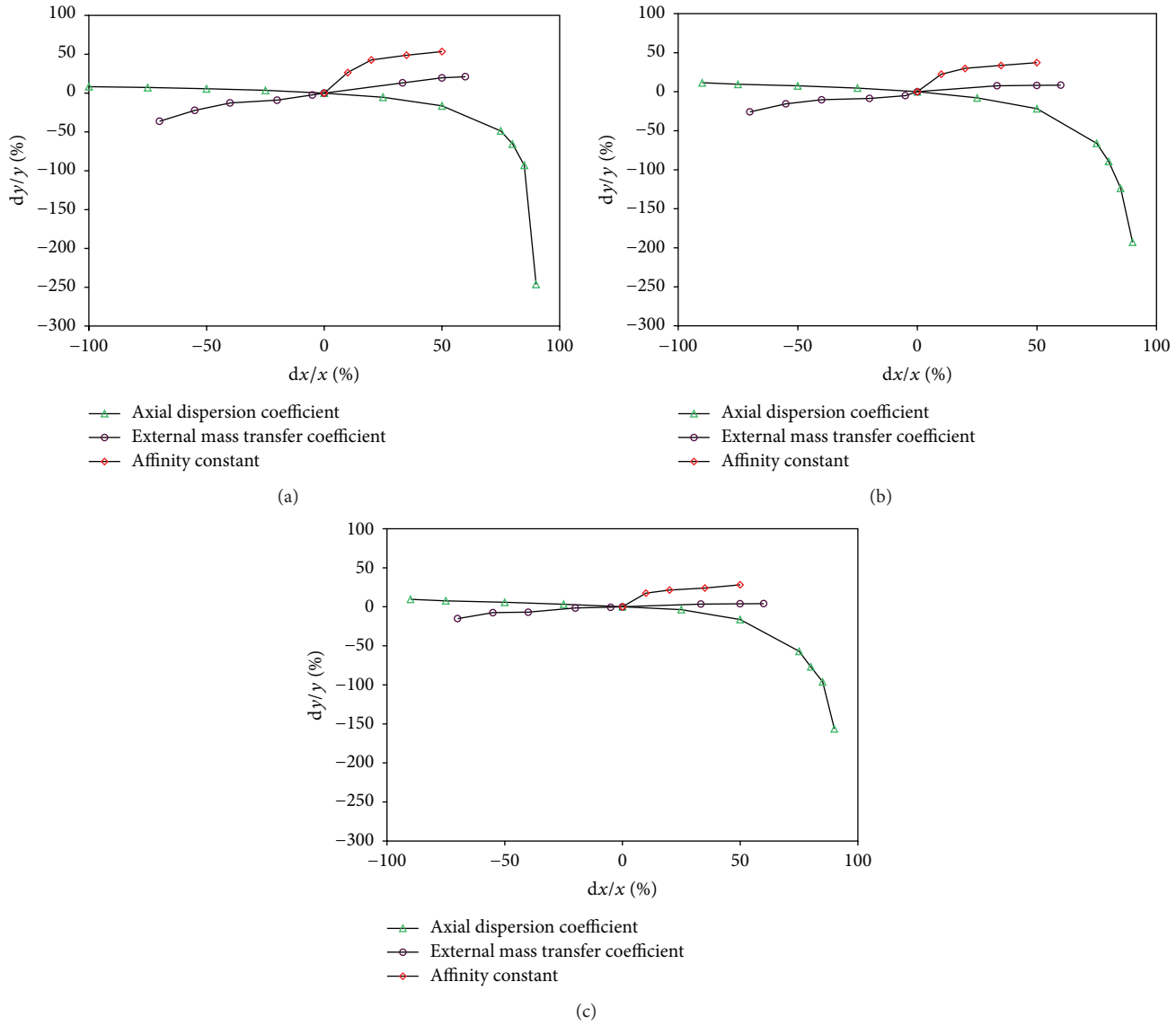

Figure 9: Sensitivity analysis of the mass transfer model for the adsorption of (a) Cd^{2+}, (b) Cu^{2+}, and (c) Pb^{2+} onto SCG.

the active sites on SCG surface. The spent coffee ground was able to remove heavy metal from synthetic multicomponent solutions. However, the presence of other contaminants could be detrimental to the adsorption capacity in multicomponent systems and further investigations need to be performed with multicomponent real solutions. Additionally, the SCG could be employed in at least four consecutive adsorption/desorption cycles with no loss of the heavy metal adsorption capacity using nitric acid as eluent. The breakthrough curves could be well predicted by modeling that assumed axial dispersion effect, external mass transfer resistance, and ion-exchange isotherm as rate controlling. The mass transfer model was tested for a 14 cm long adsorption column and could predict well the behavior of heavy metal adsorption onto spent coffee ground. The sensitivity analysis showed that axial dispersion is the most significant parameter in the simulation of the breakthrough curves.

Competing Interests

The authors declare that there are no competing interests regarding the publication of this paper.

Acknowledgments

The authors are grateful to the Facultad de Ciencias Químicas de la Universidad Autónoma de Nuevo León and the Consejo Nacional de Ciencia y Tecnología (CONACYT) for the financial support provided (Project Ciencia Básica 2007, no. 79746). Additionally, the authors acknowledge Professor Luz

Margarita Ramírez Vigil for her technical support to this research.

References

[1] M. Sprynskyy, B. Buszewski, A. P. Terzyk, and J. Namieśnik, "Study of the selection mechanism of heavy metal (Pb^{2+}, Cu^{2+}, Ni^{2+}, and Cd^{2+}) adsorption on clinoptilolite," *Journal of Colloid and Interface Science*, vol. 304, no. 1, pp. 21–28, 2006.

[2] R. O. Cañizares-Villanueva, "Biosorción de metales pesados mediante el uso de biomasa microbiana," *Revista Latinoamericana de Microbiología*, vol. 42, pp. 131–143, 2000.

[3] F. Pagnanelli, A. Esposito, and F. Vegliò, "Multi-metallic modelling for biosorption of binary systems," *Water Research*, vol. 36, no. 16, pp. 4095–4105, 2002.

[4] United States Department of Agriculture, *Coffee: World Markets and Trade*, 2015, http://apps.fas.usda.gov/psdonline/circulars/coffee.pdf.

[5] N. E. Dávila-Guzmán, F. De Jesús Cerino-Cordova, E. Soto-Regalado et al., "Copper biosorption by spent coffee ground: equilibrium, kinetics, and mechanism," *Clean—Soil, Air, Water*, vol. 41, no. 6, pp. 557–564, 2013.

[6] H. D. Utomo and K. A. Hunter, "Particle concentration effect: adsorption of divalent metal ions on coffee grounds," *Bioresource Technology*, vol. 101, no. 5, pp. 1482–1486, 2010.

[7] T. Tokimoto, N. Kawasaki, T. Nakamura, J. Akutagawa, and S. Tanada, "Removal of lead ions in drinking water by coffee grounds as vegetable biomass," *Journal of Colloid and Interface Science*, vol. 281, no. 1, pp. 56–61, 2005.

[8] D. O. Cooney, A. Nagerl, and A. L. Hines, "Solvent regeneration of activated carbon," *Water Research*, vol. 17, no. 4, pp. 403–410, 1983.

[9] D. O. Cooney, *Adsorption Design for Wastewater Treatment*, CRC Press, 1998, https://books.google.com/books?id=jS3BVK-1T3iIC&pgis=1.

[10] M. J. DeMarco, A. K. SenGupta, and J. E. Greenleaf, "Arsenic removal using a polymeric/inorganic hybrid sorbent," *Water Research*, vol. 37, no. 1, pp. 164–176, 2003.

[11] V. Diniz, M. E. Weber, B. Volesky, and G. Naja, "Column biosorption of lanthanum and europium by Sargassum," *Water Research*, vol. 42, no. 1-2, pp. 363–371, 2008.

[12] A. Leusch, Z. Holan, and B. Volesky, "Biosorption of heavy metals (Cd, Cu, Ni, Pb, Zn) by chemically-reinforced biomass of marine algae," *Journal of Chemical Technology and Biotechnology*, vol. 62, no. 3, pp. 279–288, 1995.

[13] B. E. Poling, J. M. Prausnitz, and J. P. O'Connell, *The Properties of Gases and Liquids*, McGraw-Hill, 2001, https://books.google.com.mx/books/about/The_properties_of_gases_and_liquids.html?id=s_NUAAAAMAAJ&pgis=1.

[14] J. M. P. Q. Delgado, "A critical review of dispersion in packed beds," *Heat and Mass Transfer*, vol. 42, no. 4, pp. 279–310, 2006.

[15] M. Steiner, W. Pronk, and M. A. Boller, "Modeling of copper sorption onto GFH and design of full-scale GFH adsorbers," *Environmental Science and Technology*, vol. 40, no. 5, pp. 1629–1635, 2006.

[16] L. Lv, Y. Zhang, K. Wang, A. K. Ray, and X. S. Zhao, "Modeling of the adsorption breakthrough behaviors of Pb^{2+} in a fixed bed of ETS-10 adsorbent," *Journal of Colloid and Interface Science*, vol. 325, no. 1, pp. 57–63, 2008.

[17] A. Hatzikioseyian, F. Mavituna, and M. Tsezos, "Modelling of fixed bed biosorption columns in continuous metal ion removal processes. The case of single solute local equilibrium," *Process Metallurgy*, vol. 9, pp. 429–448, 1999.

[18] H. An, "Crab shell for the removal of heavy metals from aqueous solution," *Water Research*, vol. 35, no. 15, pp. 3551–3556, 2001.

[19] E. Pehlivan and T. Altun, "The study of various parameters affecting the ion exchange of Cu^{2+}, Zn^{2+}, Ni^{2+}, Cd^{2+}, and Pb^{2+} from aqueous solution on Dowex 50W synthetic resin," *Journal of Hazardous Materials*, vol. 134, no. 1–3, pp. 149–156, 2006.

[20] W. M. Hanynes, *CRC Handbook of Chemistry and Physics*, CRC Press, 93rd edition, 2012, https://books.google.com.mx/books/about/CRC_Handbook_of_Chemistry_and_Physics_93.html?id=-BzP7Rkl7WkC&pgis=1.

[21] S. Srivastava and P. Goyal, *Novel Biomaterials*, Springer, Berlin, Germany, 2010.

[22] S. Lukman, M. H. Essa, N. D. Mu'azu, A. Bukhari, and C. Basheer, "Adsorption and desorption of heavy metals onto natural clay material: influence of initial pH," *Journal of Environmental Science and Technology*, vol. 6, no. 1, pp. 1–15, 2013.

[23] Official Mexican Norm NOM-003-ECOL-1997, It establishes the maximum pollution limits for the reuse of treated wastewater, 1998, http://www.ordenjuridico.gob.mx/Documentos/Federal/wo69207.pdf.

[24] J. M. P. Q. Delgado, "Longitudinal and transverse dispersion in porous media," *Chemical Engineering Research and Design*, vol. 85, no. 9, pp. 1245–1252, 2007.

[25] F. J. Cerino-Córdova, P. E. Díaz-Flores, R. B. García-Reyes et al., "Biosorption of Cu(II) and Pb(II) from aqueous solutions by chemically modified spent coffee grains," *International Journal of Environmental Science and Technology*, vol. 10, no. 3, pp. 611–622, 2013.

[26] A. Demirbas, E. Pehlivan, F. Gode, T. Altun, and G. Arslan, "Adsorption of Cu(II), Zn(II), Ni(II), Pb(II), and Cd(II) from aqueous solution on Amberlite IR-120 synthetic resin," *Journal of Colloid and Interface Science*, vol. 282, no. 1, pp. 20–25, 2005.

[27] J. Hur, J. Shin, J. Yoo, and Y.-S. Seo, "Competitive adsorption of metals onto magnetic graphene oxide: comparison with other carbonaceous adsorbents," *Scientific World Journal*, vol. 2015, Article ID 836287, 11 pages, 2015.

[28] B. M. W. P. K. Amarasinghe and R. A. Williams, "Tea waste as a low cost adsorbent for the removal of Cu and Pb from wastewater," *Chemical Engineering Journal*, vol. 132, no. 1–3, pp. 299–309, 2007.

[29] T. Bohli, "Comparative study of bivalent cationic metals adsorption Pb(II), Cd(II), Ni(II) and Cu(II) on olive stones chemically activated carbon," *Journal of Chemical Engineering & Process Technology*, vol. 04, no. 04, 2013.

[30] M. Minamisawa, H. Minamisawa, S. Yoshida, and N. Takai, "Adsorption behavior of heavy metals on biomaterials," *Journal of Agricultural and Food Chemistry*, vol. 52, no. 18, pp. 5606–5611, 2004.